INTERNATIONAL JOURNAL OF
NUMERICAL ANALYSIS AND MODELING
Volume 11, Number 4, Pages 715–725

ANALYSIS OF THE DISCONTINUOUS GALERKIN INTERIOR PENALTY METHOD WITH SOLENOIDAL APPROXIMATIONS FOR THE STOKES EQUATIONS

ADELINE MONTLAUR AND SONIA FERNANDEZ-MENDEZ

Abstract. The discontinuous Galerkin Interior Penalty Method with solenoidal approximations proposed in [13] for the incompressible Stokes equations is analyzed. Continuity and coercivity of the bilinear form are proved. A priori error estimates, with optimal convergence rates, are derived. 2D and 3D numerical examples with known analytical solution corroborate the theoretical analysis.

Key words. Discontinuous Galerkin, Stokes equations, incompressible flow, divergence-free, Interior Penalty Method, error bounds.

1. Introduction

Discontinuous Galerkin (DG) methods have become very popular for incompressible flow problems, especially in combination with piecewise solenoidal approximations [2, 4, 5, 7, 12, 13, 14, 15]. In the context of conforming finite elements, solenoidal approximations were derived by Crouzeix and Raviart in [6], allowing one to obtain a formulation involving only velocity. Nevertheless their implementation is non-trivial and they are limited to low-order approximations. While alternative solutions for incompressible flows are, among others, velocity-pressure formulations satisfying the Babuska-Brezzi condition, or *hp*-version FEM, in a DG framework high-order solenoidal approximations can be easily defined. This leads to an important saving in the number of degrees of freedom, with the corresponding reduction in computational cost, see [16].

Cockburn and collaborators [4, 5] were among the first researchers to use solenoidal approximations for incompressible flows in the context of the Local Discontinuous Galerkin (LDG) method, and they also introduced the concept of hybrid pressure. Later, the use of solenoidal approximations and hybrid pressure has been applied to an Interior Penalty Method (IPM), in [13], and to a Compact Discontinuous Galerkin (CDG) method, see [16, 17]. In [13], the velocity approximation space is decomposed in every element into a solenoidal part and an irrotational part. This allows for a splitting of the original weak form in two uncoupled problems. The first one solves for velocity and hybrid pressure, and the second one allows evaluating the pressure in the interior of the elements, as a post-processing of the velocity solution.

LDG, CDG and IPM methods all lead to symmetric and coercive bilinear forms for self-adjoint operators. But IPM and CDG methods have the major advantage, relative to LDG, of being compact formulations, that is, the degrees of freedom of one element are only connected to those of immediate neighbors. In [16], IPM and CDG methods are further compared for the solution of the Navier-Stokes equations.

Received by the editors November 11, 2012 and, in revised form, February 2, 2014.
2000 *Mathematics Subject Classification.* 35Q35, 65G99, 76D07.
This work has been supported by the Generalitat de Catalunya (AGAUR), 2009SGR875 and by the Network for Initial Training FP7-PEOPLE-ITN-2008, Advanced Techniques in Computational Mechanics PITN-GA-2009-238548.

Both methods present similar results for the accuracy of the numerical solution, reaching optimal convergence rates for velocity and pressure. The main differences are that CDG is less sensitive to the selection of the penalty parameter, but has the major disadvantage of the implementation and computation of the lifting operators. The liftings, introduced in CDG [17] as well as in LDG [4], also induce an approximate orthogonality property and a loss of consistency, whereas IPM is a consistent formulation with a straight-forward implementation.

This paper performs a complete analysis of the discontinuous Galerkin IPM (DG-IPM) with solenoidal approximations and hybrid pressure, as derived and applied to 2D examples in [13], for the incompressible Stokes equations. Standard properties of continuity and coercivity of the obtained weak form are proved. The error estimate for velocity proved in [13] is recalled, and a new error estimate is derived for the post-processed interior pressure, in the case of pure Dirichlet boundary conditions. Some intermediate results from [4, 12] are used in these demonstrations and derivations. All demonstrations in this paper are proved for any spatial dimension (either triangles in 2D or tetrahedra in 3D), except for the unique solvability of the IPM problem, which is only considered for the 2D case.

The paper is structured as follows. The IPM formulation, with a splitting of the velocity space into solenoidal and irrotational parts, is summarized in Section 2 for the solution of the incompressible Stokes equations. Various properties of the IPM formulation are then presented and proved in Section 3. In particular, standard properties of continuity and coercivity of the bilinear form are proved, the error bound for velocity is recalled and a new error bound for interior pressure is derived. 2D and 3D numerical examples with analytical solutions validate the theoretical analysis in Section 4.

2. Discontinuous Galerkin interior penalty formulation for Stokes

Let $\Omega \subset \mathbb{R}^{\mathtt{n_{sd}}}$ be an open bounded domain with boundary $\partial\Omega$ and $\mathtt{n_{sd}}$ the number of spatial dimensions. Suppose that Ω is partitioned in $\mathtt{n_{el}}$ disjoint subdomains Ω_i, triangles in 2D or tetrahedral elements in 3D, with boundaries $\partial\Omega_i$ that define an internal interface Γ; the following definitions and notation are used

$$\overline{\Omega} = \bigcup_{i=1}^{\mathtt{n_{el}}} \overline{\Omega}_i, \quad \Omega_i \cap \Omega_j = \emptyset \text{ for } i \neq j,$$

$$\text{and } \Gamma := \bigcup_{\substack{i,j=1 \\ i\neq j}}^{\mathtt{n_{el}}} \overline{\Omega}_i \cap \overline{\Omega}_j = \Big[\bigcup_{i=1}^{\mathtt{n_{el}}} \partial\Omega_i\Big] \backslash \partial\Omega.$$

The strong form for the steady incompressible Stokes problem can be written as

$$-\boldsymbol{\nabla}\cdot\boldsymbol{\sigma} = \boldsymbol{s} \qquad \text{in } \Omega, \tag{1a}$$

$$\boldsymbol{\nabla}\cdot\boldsymbol{u} = 0 \qquad \text{in } \Omega, \tag{1b}$$

$$\boldsymbol{u} = \boldsymbol{u}_D \qquad \text{on } \Gamma_D, \tag{1c}$$

where $\Gamma_D = \partial\Omega$, $\boldsymbol{s} \in \mathcal{L}_2(\Omega)$ is a source term, and $\boldsymbol{\sigma}$ is the ("dynamic" or "density-scaled") Cauchy stress, which is related to velocity $\boldsymbol{u}$, and pressure p, by the linear Stokes' law

$$\boldsymbol{\sigma} = -p\,\mathbf{I} + 2\nu\,\boldsymbol{\nabla}^{\mathbf{s}}\boldsymbol{u}, \tag{2}$$

with ν being the kinematic viscosity and $\boldsymbol{\nabla}^{\mathbf{s}} = \frac{1}{2}(\boldsymbol{\nabla} + \boldsymbol{\nabla}^T)$.

Note that, for a Dirichlet problem, the usual compatibility condition must be satisfied, that is $\int_{\partial\Omega} \boldsymbol{u}_D \cdot \boldsymbol{n} d\Gamma = 0$. Furthermore, an additional equation is needed in order to close the problem. For instance, pressure mean value can be set to zero.

The *jump* $[\![\cdot]\!]$ and *mean* $\{\cdot\}$ operators are defined along the interface Γ using values from the elements to the left and to the right of the interface (say, Ω_i and Ω_j) and are also extended along the exterior boundary (only values in Ω are employed), namely

$$[\![\circledcirc]\!] = \begin{cases} \circledcirc_i + \circledcirc_j & \text{on } \Gamma, \\ \circledcirc & \text{on } \partial\Omega, \end{cases} \quad \text{and} \quad \{\circledcirc\} = \begin{cases} \kappa_i \circledcirc_i + \kappa_j \circledcirc_j & \text{on } \Gamma, \\ \circledcirc & \text{on } \partial\Omega. \end{cases}$$

Usually $\kappa_i = \kappa_j = 1/2$ but, in general, these two scalars are only required to verify $\kappa_i + \kappa_j = 1$, see for instance [10]. The major difference between the mean and the jump operator is that the latter always involves the normal to the interface or to the domain. For instance, given two adjacent subdomains Ω_i and Ω_j, their exterior unit normals are denoted respectively $\boldsymbol{n}_i$ and $\boldsymbol{n}_j$ (recall that $\boldsymbol{n}_i = -\boldsymbol{n}_j$) and along $\partial\Omega$ the exterior unit normal is denoted by $\boldsymbol{n}$; the jump is then

$$[\![p\,\boldsymbol{n}]\!] = \begin{cases} p_i\,\boldsymbol{n}_i + p_j\,\boldsymbol{n}_j = \boldsymbol{n}_i(p_i - p_j) & \text{on } \Gamma \\ p\,\boldsymbol{n} & \text{on } \partial\Omega \end{cases}$$

for scalars, see [13] for vectors or tensors.

Finally, in the following equations, $(\cdot,\cdot)$ denotes the $\mathcal{L}_2$-scalar product in Ω, that is

$$(p,q) = \sum_{\Omega_i \in \Omega} \int_{\Omega_i} p\,q\,d\Omega \qquad \text{for scalars,} \tag{3a}$$

$$(\boldsymbol{u},\boldsymbol{v}) = \sum_{\Omega_i \in \Omega} \int_{\Omega_i} \boldsymbol{u}\cdot\boldsymbol{v}\,d\Omega \qquad \text{for vectors,} \tag{3b}$$

$$(\boldsymbol{\sigma},\boldsymbol{\tau}) = \sum_{\Omega_i \in \Omega} \int_{\Omega_i} \boldsymbol{\sigma} : \boldsymbol{\tau}\,d\Omega \qquad \text{for second-order tensors} \tag{3c}$$

where all the integrals are considered element-wise. Similarly, derivative operators applied to discontinuous but piecewise smooth functions are understood in an element-wise sense.

Analogously, $(\cdot,\cdot)_\Upsilon$ denotes the $\mathcal{L}_2$-scalar product in any domain $\Upsilon \subset \Gamma \cup \partial\Omega$. For instance,

$$(p,q)_\Upsilon = \int_\Upsilon p\,q\,d\Gamma \tag{4}$$

for scalars.

2.1. IPM formulation. The following discrete finite element spaces for velocity and pressure are defined

$$\begin{aligned} \boldsymbol{\mathcal{V}}^h &= \{\boldsymbol{v} \in [\mathcal{L}_2(\Omega)]^{\mathtt{n_{sd}}} \,;\; \boldsymbol{v}|_{\Omega_i} \in [\mathcal{P}^k(\Omega_i)]^{\mathtt{n_{sd}}} \quad \forall \Omega_i\} \\ \mathcal{Q}^h &= \{q \in [\mathcal{L}_2(\Omega)] \,;\; q|_{\Omega_i} \in [\mathcal{P}^{k-1}(\Omega_i)] \quad \forall \Omega_i\} \end{aligned} \tag{5}$$

where $\mathcal{P}^k(\Omega_i)$ is the space of polynomial functions of degree at most k in Ω_i, with some fixed approximation degree $k \geq 1$.

Following the standard approach of Interior Penalty Method, introduced by [1] for second-order parabolic equations, the Interior Penalty approach developed by

[13] for the Stokes equations is: find $\boldsymbol{u}_h \in \boldsymbol{\mathcal{V}}^h$ and $p_h \in \mathcal{Q}^h/\mathbb{R}$ such that

$$
\begin{aligned}
a\big(\boldsymbol{u}_h, \boldsymbol{v}\big) + b\big(\boldsymbol{v}, p_h\big) + \big(\{p_h\}, [\![\boldsymbol{n}\cdot\boldsymbol{v}]\!]\big)_{\Gamma\cup\Gamma_D} &= l\big(\boldsymbol{v}\big) && \forall\, \boldsymbol{v} \in \boldsymbol{\mathcal{V}}^h,\\
b\big(\boldsymbol{u}_h, q\big) + \big(\{q\}, [\![\boldsymbol{n}\cdot\boldsymbol{u}_h]\!]\big)_{\Gamma\cup\Gamma_D} &= \big(q, \boldsymbol{n}\cdot\boldsymbol{u}_D\big)_{\Gamma_D} && \forall\, q \in \mathcal{Q}^h/\mathbb{R},
\end{aligned}
\tag{6}
$$

where

$$
\begin{aligned}
a\big(\boldsymbol{u}, \boldsymbol{v}\big) := \big(2\nu\boldsymbol{\nabla}^{\mathtt{S}}\boldsymbol{u}, \boldsymbol{\nabla}^{\mathtt{S}}\boldsymbol{v}\big) + \frac{\gamma}{h}\big([\![\boldsymbol{n}\otimes\boldsymbol{u}]\!], [\![\boldsymbol{n}\otimes\boldsymbol{v}]\!]\big)_{\Gamma\cup\Gamma_D}\\
- \big(2\nu\{\boldsymbol{\nabla}^{\mathtt{S}}\boldsymbol{u}\}, [\![\boldsymbol{n}\otimes\boldsymbol{v}]\!]\big)_{\Gamma\cup\Gamma_D} - \big([\![\boldsymbol{n}\otimes\boldsymbol{u}]\!], 2\nu\{\boldsymbol{\nabla}^{\mathtt{S}}\boldsymbol{v}\}\big)_{\Gamma\cup\Gamma_D},
\end{aligned}
\tag{7a}
$$

$$
l\big(\boldsymbol{v}\big) := \big(\boldsymbol{f}, \boldsymbol{v}\big) + \frac{\gamma}{h}\big(\boldsymbol{u}_D, \boldsymbol{v}\big)_{\Gamma_D} - \big(\boldsymbol{n}\otimes\boldsymbol{u}_D, 2\nu\boldsymbol{\nabla}^{\mathtt{S}}\boldsymbol{v}\big)_{\Gamma_D},
\tag{7b}
$$

$$
b\big(\boldsymbol{v}, p\big) := -\int_\Omega p\,\boldsymbol{\nabla}\cdot\boldsymbol{v}\,d\Omega.
\tag{7c}
$$

The characteristic mesh size is denoted by h. For instance, following [11], for a 2D mesh of straight sides, the mesh parameter h can be defined on each side $\partial\Omega_i$, interface between two elements Ω_i and Ω_j or on the boundary $\partial\Omega$, by

$$
h_{|\partial\Omega_i} = \begin{cases} 2\left(\dfrac{\text{length}(\partial\Omega_i)}{\text{area}(\Omega_i)} + \dfrac{\text{length}(\partial\Omega_i)}{\text{area}(\Omega_j)}\right)^{-1} & \text{for } \partial\Omega_i \text{ on } \Gamma,\\[2ex] \dfrac{\text{area}(\Omega_i)}{\text{length}(\partial\Omega_i)} & \text{for } \partial\Omega_i \text{ on } \partial\Omega. \end{cases}
\tag{8}
$$

Another possibility, in 2D as well as in 3D problems, is to consider h equal to the minimum length of the sides of an element. The penalty parameter γ is a positive scalar, depending on ν and k, which must be large enough to ensure the coercivity of the symmetric bilinear form $a\big(.,.\big)$, see [13] and Section 4.

2.2. IPM with solenoidal approximations. The velocity space $\boldsymbol{\mathcal{V}}^h$ is now split into the direct sum of a solenoidal part and an irrotational part, see [13, 5, 4] for details, that is $\boldsymbol{\mathcal{V}}^h = \boldsymbol{\mathcal{S}}^h \oplus \boldsymbol{\mathcal{I}}^h$, where

$$
\begin{aligned}
\boldsymbol{\mathcal{S}}^h &= \big\{\boldsymbol{v} \in \boldsymbol{\mathcal{V}}^h \mid \boldsymbol{\nabla}\cdot\boldsymbol{v}|_{\Omega_i} = 0 \text{ for } i = 1, \ldots, \mathtt{n_{el}}\big\},\\
\boldsymbol{\mathcal{I}}^h &\subset \big\{\boldsymbol{v} \in \boldsymbol{\mathcal{V}}^h \mid \boldsymbol{\nabla}\times\boldsymbol{v}|_{\Omega_i} = \boldsymbol{0} \text{ for } i = 1, \ldots, \mathtt{n_{el}}\big\}.
\end{aligned}
\tag{9}
$$

For instance, a solenoidal basis in a 2D triangle for an approximation of degree $k = 2$ is

$$
\boldsymbol{\mathcal{S}}^h = \left\langle \begin{pmatrix} 1\\0 \end{pmatrix}, \begin{pmatrix} 0\\1 \end{pmatrix}, \begin{pmatrix} 0\\x \end{pmatrix}, \begin{pmatrix} x\\-y \end{pmatrix}, \begin{pmatrix} y\\0 \end{pmatrix}, \begin{pmatrix} 0\\x^2 \end{pmatrix}, \begin{pmatrix} 2xy\\-y^2 \end{pmatrix}, \begin{pmatrix} x^2\\-2xy \end{pmatrix}, \begin{pmatrix} y^2\\0 \end{pmatrix} \right\rangle,
$$

and the irrotational complementary part for $k = 2$ is

$$
\boldsymbol{\mathcal{I}}^h = \left\langle \begin{pmatrix} x\\0 \end{pmatrix}, \begin{pmatrix} x^2\\0 \end{pmatrix}, \begin{pmatrix} 0\\y^2 \end{pmatrix} \right\rangle,
$$

see for example [2] for the construction of these spaces.

Under these circumstances, the IPM problem (6) can be split in two *uncoupled* problems. The first one solves for *divergence-free* velocities and the so-called *hybrid*

pressures: find $\boldsymbol{u}_h \in \boldsymbol{\mathcal{S}}^h$ and $\tilde{p}_h \in \boldsymbol{P}^h/\mathbb{R}$ solution of

$$\text{(10a)} \qquad \begin{cases} a\big(\boldsymbol{u}_h, \boldsymbol{v}\big) + \big(\tilde{p}_h, [\![\boldsymbol{n}\cdot\boldsymbol{v}]\!]\big)_{\Gamma\cup\Gamma_D} = l\big(\boldsymbol{v}\big) & \forall \boldsymbol{v} \in \boldsymbol{\mathcal{S}}^h, \\ \big(\tilde{q}, [\![\boldsymbol{n}\cdot\boldsymbol{u}_h]\!]\big)_{\Gamma\cup\Gamma_D} = \big(\tilde{q}, \boldsymbol{n}\cdot\boldsymbol{u}_D\big)_{\Gamma_D} & \forall \tilde{q} \in \boldsymbol{P}^h/\mathbb{R}, \end{cases}$$

with the form $a\big(.,.\big)$ defined in (7).

The space of hybrid pressures (pressures along the sides in 2D, or faces in 3D) is simply:

$$\boldsymbol{P}^h := \left\{ \tilde{p} \mid \tilde{p} : \Gamma \cup \Gamma_D \longrightarrow \mathbb{R} \ \text{ and } \ \tilde{p} = [\![\boldsymbol{n}\cdot\boldsymbol{v}]\!] \ \text{ for some } \ \boldsymbol{v} \in \boldsymbol{\mathcal{S}}^h \right\}.$$

In fact, [5] demonstrates that $\boldsymbol{P}^h$ corresponds to piecewise polynomial pressures on the element sides in 2D or faces in 3D.

Remark 1. *The proof of the unique solvability of* (10a) *can be established in 2D following* [4]. *An analogous result in 3D remains an open issue and is beyond the scope of this paper. Note that numerical 3D results, see Section 4, do not indicate any problems to that extent.*

The second problem, which requires the solution $(\boldsymbol{u}_h, \tilde{p}_h)$ of (10a), evaluates the *interior pressures*: find $p_h \in \mathcal{Q}^h$ such that

$$\text{(10b)} \qquad b\big(\boldsymbol{v}, p_h\big) = l\big(\boldsymbol{v}\big) - a\big(\boldsymbol{u}_h, \boldsymbol{v}\big) - \big(\tilde{p}_h, [\![\boldsymbol{n}\cdot\boldsymbol{v}]\!]\big)_{\Gamma\cup\Gamma_D} \quad \forall \boldsymbol{v} \in \boldsymbol{\mathcal{I}}^h.$$

It is important to note that equation (10b) is a post-processing of the solution of (10a), with an element by element computation.

3. Analysis of IPM with solenoidal approximations

This section presents the standard continuity and coercivity properties of the IPM bilinear form (7a) and the error bounds for the IPM Stokes formulation with solenoidal velocity (10). To that end, the $|||\cdot|||$-norm is defined as

$$\text{(11)} \qquad |||\boldsymbol{v}|||^2 = \|\boldsymbol{\nabla}^{\mathbf{s}}\boldsymbol{v}\|_\Omega^2 + \|h^{1/2}\{\boldsymbol{\nabla}^{\mathbf{s}}\boldsymbol{v}\}\|_{\Gamma\cup\Gamma_D}^2 + \|h^{-1/2}[\![\boldsymbol{n}\otimes\boldsymbol{v}]\!]\|_{\Gamma\cup\Gamma_D}^2$$

with the $\mathcal{L}_2$-norms induced by the scalar products (3) and (4)

$$\text{(12)} \qquad \|f\|_\Omega^2 = \big(f, f\big) \qquad \text{and} \qquad \|f\|_{\Gamma\cup\Gamma_D}^2 = \big(f, f\big)_{\Gamma\cup\Gamma_D}.$$

Note that, given the element-wise integration in the definition of the $\mathcal{L}_2$-scalar products in (3) and (4), these $\mathcal{L}_2$-norms also involve element-wise integrals, allowing their application to discontinuous functions.

The steps used here to prove the continuity and coercivity of $a\big(.,.\big)$ are similar to the ones followed in [12], also for the Stokes equations, using some properties proved in [11], for an elasticity problem. Note that in [12], an alternative IPM formulation is derived, the main difference with the method analyzed here being the presence of a non-consistent penalty parameter, which leads to a formulation with no pressure at all.

Lemma 3.1 (Continuity)**.** *The IPM bilinear form,* $a\big(.,.\big)$*, defined in* (7a) *is continuous. That is*

$$\text{(13)} \qquad |a(\boldsymbol{u}, \boldsymbol{v})| \leq C \,|||\,\boldsymbol{u}\,|||\;|||\boldsymbol{v}\,||| \quad \forall \boldsymbol{u}, \boldsymbol{v} \in \boldsymbol{\mathcal{V}}^h + \big[[\mathcal{H}^1(\Omega)]^{n_{sd}} \cap \mathcal{H}(div^0; \Omega)\big]$$

for some constant $C > 0$ *independent of the mesh size, where* $\mathcal{H}(div^0; \Omega) = \{\boldsymbol{v} \in [\mathcal{L}_2(\Omega)]^{n_{sd}} \mid \boldsymbol{\nabla}\cdot\boldsymbol{v} = 0 \text{ in } \Omega\}$.

Proof. Using the Schwarz inequality, we have

$$
\begin{aligned}
(14)\quad \big|a\big(\boldsymbol{u},\boldsymbol{v}\big)\big|^2 \leq \Big(&2\nu\|\boldsymbol{\nabla}^{\mathbf{s}}\boldsymbol{u}\|_{\Omega}\|\boldsymbol{\nabla}^{\mathbf{s}}\boldsymbol{v}\|_{\Omega}+\frac{\gamma}{h}\|[\![\boldsymbol{n}\otimes\boldsymbol{u}]\!]\|_{\Gamma\cup\Gamma_D}\|[\![\boldsymbol{n}\otimes\boldsymbol{v}]\!]\|_{\Gamma\cup\Gamma_D}\\
&+2\nu\left(\|\{\boldsymbol{\nabla}^{\mathbf{s}}\boldsymbol{u}\}\|_{\Gamma\cup\Gamma_D}\|[\![\boldsymbol{n}\otimes\boldsymbol{v}]\!]\|_{\Gamma\cup\Gamma_D}+\|[\![\boldsymbol{n}\otimes\boldsymbol{u}]\!]\|_{\Gamma\cup\Gamma_D}\|\{\boldsymbol{\nabla}^{\mathbf{s}}\boldsymbol{v}\}\|_{\Gamma\cup\Gamma_D}\right)\Big)^2\\
=4\nu^2\Big(&\|\boldsymbol{\nabla}^{\mathbf{s}}\boldsymbol{u}\|_{\Omega}^2\|\boldsymbol{\nabla}^{\mathbf{s}}\boldsymbol{v}\|_{\Omega}^2+\|\{\boldsymbol{\nabla}^{\mathbf{s}}\boldsymbol{u}\}\|_{\Gamma\cup\Gamma_D}^2\|[\![\boldsymbol{n}\otimes\boldsymbol{v}]\!]\|_{\Gamma\cup\Gamma_D}^2+\|[\![\boldsymbol{n}\otimes\boldsymbol{u}]\!]\|_{\Gamma\cup\Gamma_D}^2\|\{\boldsymbol{\nabla}^{\mathbf{s}}\boldsymbol{v}\}\|_{\Gamma\cup\Gamma_D}^2\\
&+2\left(\|\{\boldsymbol{\nabla}^{\mathbf{s}}\boldsymbol{u}\}\|_{\Gamma\cup\Gamma_D}\|[\![\boldsymbol{n}\otimes\boldsymbol{v}]\!]\|_{\Gamma\cup\Gamma_D}\|[\![\boldsymbol{n}\otimes\boldsymbol{u}]\!]\|_{\Gamma\cup\Gamma_D}\|\{\boldsymbol{\nabla}^{\mathbf{s}}\boldsymbol{v}\}\|_{\Gamma\cup\Gamma_D}\right)\Big)\\
&+\frac{\gamma^2}{h^2}\|[\![\boldsymbol{n}\otimes\boldsymbol{u}]\!]^2\|_{\Gamma\cup\Gamma_D}\|[\![\boldsymbol{n}\otimes\boldsymbol{v}]\!]^2\|_{\Gamma\cup\Gamma_D}\\
+8\nu^2\|\boldsymbol{\nabla}^{\mathbf{s}}\boldsymbol{u}\|_{\Omega}\|\boldsymbol{\nabla}^{\mathbf{s}}\boldsymbol{v}\|_{\Omega}\Big(&\|\{\boldsymbol{\nabla}^{\mathbf{s}}\boldsymbol{u}\}\|_{\Gamma\cup\Gamma_D}\|[\![\boldsymbol{n}\otimes\boldsymbol{v}]\!]\|_{\Gamma\cup\Gamma_D}+\|[\![\boldsymbol{n}\otimes\boldsymbol{u}]\!]\|_{\Gamma\cup\Gamma_D}\|\{\boldsymbol{\nabla}^{\mathbf{s}}\boldsymbol{v}\}\|_{\Gamma\cup\Gamma_D}\Big)\\
&+\frac{4\nu\gamma}{h}\|[\![\boldsymbol{n}\otimes\boldsymbol{u}]\!]\|_{\Gamma\cup\Gamma_D}\|[\![\boldsymbol{n}\otimes\boldsymbol{v}]\!]\|_{\Gamma\cup\Gamma_D}\Big(\|\boldsymbol{\nabla}^{\mathbf{s}}\boldsymbol{u}\|_{\Omega}\|\boldsymbol{\nabla}^{\mathbf{s}}\boldsymbol{v}\|_{\Omega}\\
&+\|\{\boldsymbol{\nabla}^{\mathbf{s}}\boldsymbol{u}\}\|_{\Gamma\cup\Gamma_D}\|[\![\boldsymbol{n}\otimes\boldsymbol{v}]\!]\|_{\Gamma\cup\Gamma_D}+\|[\![\boldsymbol{n}\otimes\boldsymbol{u}]\!]\|_{\Gamma\cup\Gamma_D}\|\{\boldsymbol{\nabla}^{\mathbf{s}}\boldsymbol{v}\}\|_{\Gamma\cup\Gamma_D}\Big)
\end{aligned}
$$

Each one of the terms in the right hand side of (14) can then be bounded by $c\,|||\,\boldsymbol{u}\,|||^2\,|||\boldsymbol{v}|||^2$, for some constant c, applying several times the inequality $2ab < a^2\epsilon + b^2/\epsilon$, which is true for any arbitrary constant ϵ. For example, one of the terms from (14) is bounded as follows

$$
\begin{aligned}
&\frac{4\nu\gamma}{h}\|\boldsymbol{\nabla}^{\mathbf{s}}\boldsymbol{u}\|_{\Omega}\|\boldsymbol{\nabla}^{\mathbf{s}}\boldsymbol{v}\|_{\Omega}\|[\![\boldsymbol{n}\otimes\boldsymbol{u}]\!]\|_{\Gamma\cup\Gamma_D}\|[\![\boldsymbol{n}\otimes\boldsymbol{v}]\!]\|_{\Gamma\cup\Gamma_D}\\
&\leq\frac{2\nu\gamma}{h}\left(\frac{1}{\epsilon}\|\boldsymbol{\nabla}^{\mathbf{s}}\boldsymbol{u}\|_{\Omega}^2\|\boldsymbol{\nabla}^{\mathbf{s}}\boldsymbol{v}\|_{\Omega}^2+\epsilon\|[\![\boldsymbol{n}\otimes\boldsymbol{u}]\!]\|_{\Gamma\cup\Gamma_D}^2\|[\![\boldsymbol{n}\otimes\boldsymbol{v}]\!]\|_{\Gamma\cup\Gamma_D}^2\right)\leq c|||\,\boldsymbol{u}\,|||^2|||\boldsymbol{v}|||^2,
\end{aligned}
$$

where $c = 2\nu\gamma/h\max\left(1/\epsilon,\epsilon\right)$, for any constant ϵ. □

Lemma 3.2 (Inverse inequality)**.** *For all $f\in\boldsymbol{\mathcal{V}}^h$, and any mesh parameter h (defined in* (8)*), the following inverse inequality holds*

$$
\|h^{1/2}\{f\}\|_{\Gamma\cup\Gamma_D}^2\leq C\|f\|_{\Omega}^2 \tag{15}
$$

for some constant $C>0$ independent of the mesh size.

Proof. Following finite element dimensionality and scaling from a unit reference element, see [11], we have

$$
\|h^{1/2}f\|_{\partial\Omega_i}^2\leq C\|f\|_{\Omega_i}^2, \tag{16}
$$

for some constant $C>0$ independent of the mesh size. Thus,

$$
\begin{aligned}
\|h^{1/2}\{f\}\|_{\Gamma\cup\Gamma_D}^2&\leq 2\|h^{1/2}\{f\}\|_{\Gamma}^2+\|h^{1/2}f\|_{\Gamma_D}^2=\sum_{i=1}^{\mathtt{n_{el}}}\|h^{1/2}f\|_{\partial\Omega_i}^2\\
&\leq C\sum_{i=1}^{\mathtt{n_{el}}}\|f\|_{\Omega_i}^2=C\|f\|_{\Omega}^2.
\end{aligned}
$$

□

Lemma 3.3 (Coercivity)**.** *For $\gamma>0$ large enough, the IPM bilinear form $a\big(.,.\big)$ defined in* (7a) *is coercive. That is, there exists a constant $m>0$ such that*

$$
m\,|||\,\boldsymbol{v}\,|||^2\leq a\big(\boldsymbol{v},\boldsymbol{v}\big)\quad\forall\boldsymbol{v}\in\boldsymbol{\mathcal{V}}^h. \tag{17}
$$

Proof. In fact, we will prove that given any $m > 0$, there exists a $\gamma(m) > 0$ such that (17) is verified. From definitions (7a) and (11), we have

$$a(\boldsymbol{v},\boldsymbol{v}) - m \,|||\, \boldsymbol{v} \,|||^2 = (2\nu - m)\|\boldsymbol{\nabla}^{\mathbf{s}}\boldsymbol{v}\|_\Omega^2 + (\gamma - m)\|h^{-1/2}[\![\boldsymbol{n}\otimes\boldsymbol{v}]\!]\|_{\Gamma\cup\Gamma_D}^2 - m\|h^{1/2}\{\boldsymbol{\nabla}^{\mathbf{s}}\boldsymbol{v}\}\|_{\Gamma\cup\Gamma_D}^2 - 2\big(2\nu\{\boldsymbol{\nabla}^{\mathbf{s}}\boldsymbol{v}\}, [\![\boldsymbol{n}\otimes\boldsymbol{v}]\!]\big)_{\Gamma\cup\Gamma_D}. \tag{18}$$

for any constant $m > 0$.

The third term in the right-hand-side of (18) is bounded using Lemma 3.2. That is,

$$\|h^{1/2}\{\boldsymbol{\nabla}^{\mathbf{s}}\boldsymbol{v}\}\|_{\Gamma\cup\Gamma_D}^2 \le C\|\boldsymbol{\nabla}^{\mathbf{s}}\boldsymbol{v}\|_\Omega^2, \tag{19}$$

for some constant $C > 0$ independent of the mesh size.

On the other hand, the last term in (18) is bounded using the Cauchy-Schwarz inequality and (19)

$$\begin{aligned}\big(2\nu\{\boldsymbol{\nabla}^{\mathbf{s}}\boldsymbol{v}\}, [\![\boldsymbol{n}\otimes\boldsymbol{v}]\!]\big)_{\Gamma\cup\Gamma_D} &\le 2\nu\|h^{1/2}\{\boldsymbol{\nabla}^{\mathbf{s}}\boldsymbol{v}\}\|_{\Gamma\cup\Gamma_D}\|h^{-1/2}[\![\boldsymbol{n}\otimes\boldsymbol{v}]\!]\|_{\Gamma\cup\Gamma_D}\\ &\le 2\nu C\|\boldsymbol{\nabla}^{\mathbf{s}}\boldsymbol{v}\|_\Omega\|h^{-1/2}[\![\boldsymbol{n}\otimes\boldsymbol{v}]\!]\|_{\Gamma\cup\Gamma_D}.\end{aligned}$$

Thus, using the inequality $2ab < a^2\epsilon + b^2/\epsilon$ for an arbitrary constant ϵ, the last term in (18) is bounded by

$$\big(2\nu\{\boldsymbol{\nabla}^{\mathbf{s}}\boldsymbol{v}\}, [\![\boldsymbol{n}\otimes\boldsymbol{v}]\!]\big)_{\Gamma\cup\Gamma_D} \le \frac{\nu C}{\epsilon}\|\boldsymbol{\nabla}^{\mathbf{s}}\boldsymbol{v}\|_\Omega^2 + \nu C\epsilon\|h^{-1/2}[\![\boldsymbol{n}\otimes\boldsymbol{v}]\!]\|_{\Gamma\cup\Gamma_D}^2. \tag{20}$$

Substituting (20) and (19) in (18) finally leads to

$$a(\boldsymbol{v},\boldsymbol{v}) - m \,|||\, \boldsymbol{v} \,|||^2 \ge \left(2\nu\left(1 - \frac{C}{\epsilon}\right) - m(1+C)\right)\|\boldsymbol{\nabla}^{\mathbf{s}}\boldsymbol{v}\|_\Omega^2 + (\gamma - m - 2\nu C\epsilon)\|h^{-1/2}[\![\boldsymbol{n}\otimes\boldsymbol{v}]\!]\|_{\Gamma\cup\Gamma_D}^2.$$

Thus, the coercivity is ensured if $(2\nu\,(1 - C/\epsilon) - m(1+C)) \ge 0$ and $\gamma - m - 2\nu C\epsilon \ge 0$. The first condition is satisfied if the arbitrary constant ϵ is taken $\epsilon \ge 2\nu C/(2\nu - m(1+C))$. The second condition is verified when $\gamma \ge m + 2\nu C\epsilon$, that is for γ big enough, which completes the proof of the coercivity. □

The properties of continuity and coercivity of the bilinear form $a(.,.)$ are used in the derivation of the error bounds for velocity and interior pressure coming next.

Theorem 3.4 (Velocity error bound)**.** *Let $\boldsymbol{u} \in [\mathcal{H}^{1+\alpha}(\Omega)]^{n_{sd}}$, $1 \le \alpha \le k$, be the exact velocity of the Stokes problem* (1)*, and $\boldsymbol{u}_h \in \boldsymbol{\mathcal{S}}^h$ the numerical velocity of the IPM system* (10)*, then*

$$|||\boldsymbol{u} - \boldsymbol{u}_h||| \le Kh^\alpha|\boldsymbol{u}|_{[\mathcal{H}^{1+\alpha}(\Omega)]^{n_{sd}}} \tag{21}$$

for some constant $K > 0$, independent of the mesh size h and the exact solution $\boldsymbol{u}$.

Proof. This result has been proved in [13], under the assumption of coercivity and continuity of $a(.,.)$, see Lemma 3.1 and Lemma 3.3. □

Lemma 3.5 (Equivalent norms)**.** *The $|||\cdot|||$-norm used in this work and the norm used in* [4]*, that is*

$$|||\boldsymbol{v}|||_{1,h}^2 = \|\boldsymbol{\nabla}\boldsymbol{v}\|_\Omega^2 + \|h^{-1/2}[\![\boldsymbol{n}\otimes\boldsymbol{v}]\!]\|_{\Gamma\cup\Gamma_D}^2 \tag{22}$$

are equivalent for $\boldsymbol{v} \in \boldsymbol{\mathcal{V}}^h$.

Proof. Clearly $\|\boldsymbol{v}\|_1 \leq |||\boldsymbol{v}|||$. On the other hand, using Lemma 3.2, and the inequality $\|\boldsymbol{\nabla}^{\mathtt{S}}\boldsymbol{v}\|_\Omega \leq \|\boldsymbol{\nabla}\boldsymbol{v}\|_\Omega$

$$|||\boldsymbol{v}|||^2 \leq (1+C)\|\boldsymbol{\nabla}\boldsymbol{v}\|_\Omega^2 + \|h^{-1/2}[\![\boldsymbol{n}\otimes\boldsymbol{v}]\!]\|^2_{\Gamma\cup\Gamma_D} \leq D\,|||\,\boldsymbol{v}|||^2_{1,h}$$

for $D = \max(1+C, 1)$. □

Lemma 3.6 (inf-sup condition for pressure)**.** *The spaces of velocities $\boldsymbol{\mathcal{V}}^h$ and pressures $\mathcal{Q}^h$ satisfy*

$$\sup_{\boldsymbol{v}\in\boldsymbol{\mathcal{V}}^h\cap\mathcal{H}_0(div;\Omega)} \frac{b(\boldsymbol{v},q)}{|||\boldsymbol{v}|||} \geq \beta\|P_{\mathcal{Q}^h}q\|_{\mathcal{L}_2(\Omega)/\mathbb{R}} \quad \forall q\in\mathcal{L}_2(\Omega), \tag{23}$$

for some constant $\beta>0$, independent of the characteristic mesh size h, where $P_{\mathcal{Q}^h}$ is the $\mathcal{L}_2$-projection onto $\mathcal{Q}^h$, the norm $\|.\|_{\mathcal{L}_2(\Omega)/\mathbb{R}}$ is defined as

$$\|q\|_{\mathcal{L}_2(\Omega)/\mathbb{R}} = \inf_{c\in\mathbb{R}}\|q-c\|_\Omega$$

and $\mathcal{H}_0\left(div;\Omega\right) = \{\boldsymbol{v}\in[\mathcal{L}_2(\Omega)]^{\mathtt{n_{sd}}} \mid \boldsymbol{\nabla}\cdot\boldsymbol{v}\in\mathcal{L}_2(\Omega), \boldsymbol{v}\cdot\boldsymbol{n}=0 \text{ on } \partial\Omega\}$.

A proof of this Lemma for 2D triangles can be found in Section 6.2 in [4]. The $\|\cdot\|_1$-norm is considered in [4], which is equivalent to the $|||\cdot|||$-norm as noted in Lemma 3.5. The extension of the proof to tetrahedra is straight-forward. The proof in [4] is based on the existence of a field $\tilde{\boldsymbol{v}}\in[\mathcal{H}^1_0(\Omega)]^{\mathtt{n_{sd}}}$, such that

$$b(\tilde{\boldsymbol{v}}, P_{\mathcal{Q}^h}q) \geq \|P_{\mathcal{Q}^h}q\|_{\mathcal{L}_2(\Omega)/\mathbb{R}} \quad \forall q\in\mathcal{L}_2(\Omega), \quad |||\tilde{\boldsymbol{v}}||| \leq C,$$

which is proved in Section I.5.1 in [8], and on the identity

$$b(\tilde{\boldsymbol{v}}, P_{\mathcal{Q}^h}q) = b(\boldsymbol{v}, P_{\mathcal{Q}^h}q) \quad \forall q\in\mathcal{L}_2(\Omega)$$

where $\boldsymbol{v}$ is the BDM projection of $\tilde{\boldsymbol{v}}$. The last identity can be derived, following the steps in [4], using integration by parts and the properties of the BDM projection for tetrahedra, which can be found in Section III.3.3 in [3].

Theorem 3.7 (Interior pressure error estimate)**.** *Let $\boldsymbol{u}\in[\mathcal{H}^{1+\alpha}(\Omega)]^{\mathtt{n_{sd}}}$, $1\leq\alpha\leq k$, and $p\in\mathcal{H}^\alpha(\Omega)$ be the exact solution of the Stokes problem* (1)*, $\tilde{p}=\{p\}$ on $\Gamma\cup\partial\Omega$, and $(\boldsymbol{u}_h,\tilde{p}_h,p_h)\in\boldsymbol{\mathcal{S}}^h\times\boldsymbol{P}^h/\mathbb{R}\times\mathcal{Q}^h$ the numerical solution of the IPM system* (10)*, then*

$$\|p-p_h\|_{\mathcal{L}_2(\Omega)/\mathbb{R}} \leq Kh^\alpha\left(|\boldsymbol{u}|_{[\mathcal{H}^{1+\alpha}(\Omega)]^{\mathtt{n_{sd}}}} + \|p\|_{\mathcal{H}^\alpha(\Omega)}\right) \tag{24}$$

for some constant $K>0$, independent of the mesh size h and the exact solution $(\boldsymbol{u},p)$.

Proof. The exact velocity and interior pressure $(\boldsymbol{u},p)\in[\mathcal{H}^{1+\alpha}(\Omega)]^{\mathtt{n_{sd}}}\times\mathcal{H}^\alpha(\Omega)$ solution of the Stokes problem verifies (6), that is

$$b(\boldsymbol{v},p) = l(\boldsymbol{v}) - a(\boldsymbol{u},\boldsymbol{v}) - \left(\tilde{p},[\![\boldsymbol{n}\cdot\boldsymbol{v}]\!]\right)_{\Gamma\cup\Gamma_D} \quad \forall\boldsymbol{v}\in\boldsymbol{\mathcal{V}}^h,$$

and the numerical solution $(\boldsymbol{u}_h,p_h)\in\boldsymbol{\mathcal{S}}^h\times\mathcal{Q}^h$ also verifies

$$b(\boldsymbol{v},p_h) = l(\boldsymbol{v}) - a(\boldsymbol{u}_h,\boldsymbol{v}) - \left(\tilde{p}_h,[\![\boldsymbol{n}\cdot\boldsymbol{v}]\!]\right)_{\Gamma\cup\Gamma_D} \quad \forall\boldsymbol{v}\in\boldsymbol{\mathcal{V}}^h.$$

Thus, subtracting these two equations, we have

$$b(\boldsymbol{v},p-p_h) = -a(\boldsymbol{u}-\boldsymbol{u}_h,\boldsymbol{v}) - \left(\tilde{p}-\tilde{p}_h,[\![\boldsymbol{n}\cdot\boldsymbol{v}]\!]\right)_{\Gamma\cup\Gamma_D} \quad \forall\boldsymbol{v}\in\boldsymbol{\mathcal{V}}^h.$$

In particular,

$$b(\boldsymbol{v},p-p_h) = -a(\boldsymbol{u}-\boldsymbol{u}_h,\boldsymbol{v}) \quad \forall\boldsymbol{v}\in\boldsymbol{\mathcal{V}}^h\cap\mathcal{H}_0\left(\mathrm{div};\Omega\right),$$

and using the inf-sup condition (23), we get

$$\|P_{\mathcal{Q}^h}p - p_h\|_{\mathcal{L}_2(\Omega)/\mathbb{R}} \leq \frac{\beta}{|||\boldsymbol{v}|||}\left|a\big(\boldsymbol{u}-\boldsymbol{u}_h,\boldsymbol{v}\big)\right| \quad \text{for some } \boldsymbol{v}\in\boldsymbol{\mathcal{V}}^h\cap\mathcal{H}_0\left(\mathrm{div};\Omega\right).$$

Now, using the continuity property of $a\big(.,.\big)$ in Lemma 3.1

$$\|P_{\mathcal{Q}^h}p - p_h\|_{\mathcal{L}_2(\Omega)/\mathbb{R}} \leq c\,|||\,\boldsymbol{u}-\boldsymbol{u}_h|||$$

for some constant $c>0$ independent of the mesh size, and using the velocity error bound (21) we obtain

$$\|P_{\mathcal{Q}^h}p - p_h\|_{\mathcal{L}_2(\Omega)/\mathbb{R}} \leq c' h^{\alpha}|\boldsymbol{u}|_{[\mathcal{H}^{1+\alpha}(\Omega)]^{\mathtt{n_{sd}}}}. \tag{25}$$

for some constant $c'>0$ independent of the mesh size. Eventually, given that

$$\|p-p_h\|_{\mathcal{L}_2(\Omega)/\mathbb{R}} \leq \|p-P_{\mathcal{Q}^h}p\|_{\mathcal{L}_2(\Omega)/\mathbb{R}} + \|P_{\mathcal{Q}^h}p-p_h\|_{\mathcal{L}_2(\Omega)/\mathbb{R}},$$

and given the approximation result

$$\|p-P_{\mathcal{Q}^h}p\|_{\mathcal{L}_2(\Omega)/\mathbb{R}} \leq c h^{\alpha}\|p\|_{\mathcal{H}^{\alpha}(\Omega)}$$

for some constant $c>0$ independent of the mesh size, see [4], it leads to the interior pressure error bound (24). □

4. Validating analytical examples

In this section, 2D and 3D examples with analytical solution are considered to validate the theoretical analysis from the previous section. Note that more 2D numerical examples validating the DG-IPM formulation with solenoidal approximations can also be found in [13, 16]. Here these examples are completed by a 3D study. Also, though the case with non-empty Neumann boundary conditions is not covered in the theoretical analysis, it is considered in these numerical tests, exhibiting the same behavior and optimal convergence properties. To that end, $\boldsymbol{n}\cdot\boldsymbol{\sigma}=\boldsymbol{t}$ on Γ_N, is added to the system (1), $\boldsymbol{t}$ corresponding to the boundary tractions, and in this case, $\partial\Omega = \overline{\Gamma}_D\cup\overline{\Gamma}_N$ and $\Gamma_D\cap\Gamma_N=\emptyset$. This results in the following change for the right-hand-side definition in (7b)

$$l\big(\boldsymbol{v}\big) := \big(\boldsymbol{f},\boldsymbol{v}\big) + \big(\boldsymbol{t},\boldsymbol{v}\big)_{\Gamma_N} + \frac{\gamma}{h}\big(\boldsymbol{u}_D,\boldsymbol{v}\big)_{\Gamma_D} - \big(\boldsymbol{n}\otimes\boldsymbol{u}_D, 2\nu\boldsymbol{\nabla}^{\mathtt{s}}\boldsymbol{v}\big)_{\Gamma_D}.$$

The incompressible Stokes equations with $\nu=1$ are solved in a 2D square domain $\Omega=]0,1[\times]0,1[$ with Dirichlet boundary conditions on three sides, and a Neumann boundary condition on the fourth side $\{y=0\}$, and in a 3D cubic domain $\Omega=]0,1[\times]0,1[\times]0,1[$ with Dirichlet boundary conditions on the six faces. The boundary conditions and the body force f are set to have the polynomial exact solution

$$\boldsymbol{u} = \begin{pmatrix} x^2(1-x)^2(2y-6y^2+4y^3) \\ -y^2(1-y)^2(2x-6x^2+4x^3) \end{pmatrix} \quad \text{in 2D, or}$$

$$\boldsymbol{u} = \begin{pmatrix} 4x^2(x-1)^2y(2y-1)(y-1)z(2z-1)(z-1) \\ -2y^2(y-1)^2x(2x-1)(x-1)z(2z-1)(z-1) \\ -2z^2(z-1)^2y(2y-1)(y-1)x(2x-1)(x-1) \end{pmatrix} \text{in 3D, and}$$

$$p = x(1-x) \quad \text{in 2D and 3D.}$$

Figure 1 shows the convergence under h-refinement, for uniform triangle and tetrahedral meshes. The consistent penalty parameter γ is computed using the condition

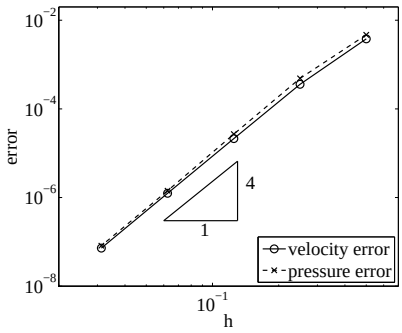

(a) 2D DG-IPM convergence results with velocity interpolation of degree 4 and pressure interpolation of degree 3.

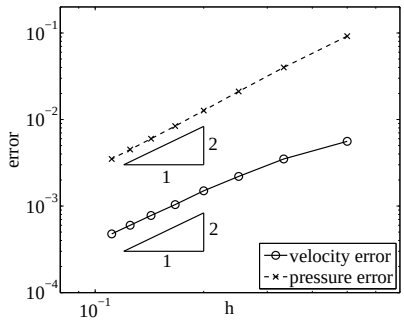

(b) 3D DG-IPM convergence results with velocity interpolation of degree 2 and pressure interpolation of degree 1.

FIGURE 1. Error convergence under h-refinement for 2D and 3D examples, with $|||\boldsymbol{.}|||$-norm for velocity and $\mathcal{L}_2$-norm for pressure.

proposed in [18] to ensure the coercivity of the bilinear form, that is

$$\gamma \approx a\nu k^2 \tag{26}$$

where a is a positive constant, determined by solving an eigenvalue problem, see [9] for more details, and k is the degree of the velocity approximation. Here $a = 2.5$ for the 2D test and $a = 10$ for the 3D test.

Both for 2D and 3D problems, the observed convergence rates of velocity and interior pressure are optimal, that is, $\boldsymbol{u}$ converges to $\boldsymbol{u}_h$ with order k for the $|||\boldsymbol{.}|||$-norm, and p converges to p_h with order k for the $\mathcal{L}_2$-norm.

5. Conclusion

This paper presents the analysis of the discontinuous Galerkin Interior Penalty Method derived for the incompressible Stokes equations and applied to 2D problems in [13]. All demonstrations in this paper are proved for any spatial dimension (either triangles in 2D or tetrahedra in 3D), except for the unique solvability of the IPM problem, which is only considered for the 2D case. Standard continuity and coercivity of the bilinear form are proved, velocity bound is recalled and a new a priori error estimate for interior pressures is derived, in the case of pure Dirichlet boundary conditions. Theoretical convergence rates are optimal for velocity and interior pressure. 2D and 3D numerical experiments validate these results.

Acknowledgments

This work has been supported by the Generalitat de Catalunya (AGAUR), 2009SGR875 and by the EC Initial Training Network PITN-GA-2009-238548.

References

[1] D. N. Arnold. An interior penalty finite element method with discontinuous elements. *SIAM J. Numer. Anal.*, 19(4):742–760, 1982.

[2] G. A. Baker, W. N. Jureidini, and O. A. Karakashian. Piecewise solenoidal vector fields and the Stokes problem. *SIAM J. Numer. Anal.*, 27(6):1466–1485, 1990.

[3] F. Brezzi and M. Fortin. *Mixed and hybrid finite element methods*, volume 15 of *Springer Series in Computational Mathematics*. Springer-Verlag, New York, 1991.

[4] J. Carrero, B. Cockburn, and D. Schötzau. Hybridized globally divergence-free LDG methods. Part I: The Stokes problem. *Math. Comp.*, 75(254):533–563, 2005.
[5] B. Cockburn and J. Gopalakrishnan. Incompressible finite elements via hybridization. Part I: the Stokes system in two space dimensions. *SIAM J. Numer. Anal.*, 43(4):1627–1650, 2005.
[6] M. Crouzeix and P.-A. Raviart. Conforming and nonconforming finite element methods for solving the stationary Stokes equations. I. *Rev. Française Automat. Informat. Recherche Opérationnelle Sér. Rouge*, 7(R-3):33–75, 1973.
[7] H. Egger and C. Waluga. A hybrid mortar method for incompressible flow. *Int. J. Numer. Anal. Model.*, 9(4):793–812, 2012.
[8] V. Girault and P.-A. Raviart. *Finite Element Approximation of the Navier-Stokes Equations*, volume 749 of *Lecture Notes in Mathematics*. Springer-Verlag, 1979.
[9] M. Griebel and M. Schweitzer. *A Particle-Partition of Unity Method-Part V: Boundary Conditions*. S. Hildebrandt and H. Karcher, editors, Geometric Analysis and Nonlinear Partial Differential Equations. Springer, Institut für Angewandte Mathematik, Universität Bonn, Wegelerstr. 6, D-53115 Bonn, Germany., 2002.
[10] A. Hansbo and P. Hansbo. A finite element method for the simulation of strong and weak discontinuities in solid mechanics. *Comput. Meth. Appl. Mech. Eng.*, 193(33-35):3523–3540, 2004.
[11] P. Hansbo and M. G. Larson. Discontinuous Galerkin methods for incompressible and nearly incompressible elasticity by Nitsche's method. *Comput. Meth. Appl. Mech. Eng.*, 191(17-18):1895–1908, 2002.
[12] P. Hansbo and M. G. Larson. Piecewise divergence-free Discontinuous Galerkin methods for Stokes flow. *Commun. Numer. Meth. Eng.*, 24(5):355–366, 2008.
[13] A. Montlaur, S. Fernandez-Mendez, and A. Huerta. Discontinuous Galerkin methods for the Stokes equations using divergence-free approximations. *Int. J. Numer. Methods Fluids*, 57(9):1071–1092, 2008.
[14] A. Montlaur, S. Fernandez-Mendez, and A. Huerta. Métodos Runge-Kutta implícitos de alto orden para flujo incompresible. *Revista Internacional Métodos numéricos para cálculo y diseño en ingeniería*, 27(1):77–91, 2011.
[15] A. Montlaur, S. Fernandez-Mendez, and A. Huerta. High-order implicit time integration for unsteady incompressible flows. *Int. J. Numer. Methods Fluids*, 70(5):603–626, 2012.
[16] A. Montlaur, S. Fernandez-Mendez, J. Peraire, and A. Huerta. Discontinuous Galerkin methods for the Navier-Stokes equations using solenoidal approximations. *Int. J. Numer. Methods Fluids*, 64(5):549–564, 2010.
[17] J. Peraire and P.-O. Persson. The Compact Discontinuous Galerkin (CDG) method for elliptic problems. *SIAM J. Sci. Stat. Comput.*, 30(4):1806–1824, 2008.
[18] S. Prudhomme, F. Pascal, J. Oden, and A. Romkes. High-order accurate time-stepping schemes for convection-diffusion problems. In *Tech. Rep. 00-27, TICAM, Austin, TX., 2000*, pages 00–27, 2000.

Escola d'Enginyeria de Telecomunicació i Aeroespacial de Castelldefels
E-mail: `adeline.de.montlaur@upc.edu`

E.T.S. d'Enginyers de Camins, Canals i Ports de Barcelona
E-mail: `sonia.fernandez@upc.edu`

Laboratori de Càlcul Numèric, Universitat Politècnica de Catalunya, Jordi Girona 1-3, 08034 Barcelona, Spain
URL: `http://www-lacan.upc.edu`